Carbohydrate Polymers 78 (2009) 60–65

Contents lists available at ScienceDirect

Carbohydrate Polymers

journal homepage: www.elsevier.com/locate/carbpol

# Preparation of nanocomposite chitosan/silk fibroin blend films containing nanopore structures

Noi Niamsa [a], Yaowalak Srisuwan [a], Yodthong Baimark [a,*], Pranee Phinyocheep [b,c], Sumet Kittipoom [c]

[a] Department of Chemistry and Center of Excellence for Innovation in Chemistry, Faculty of Science, Mahasarakham University, Mahasarakham 44150, Thailand
[b] Department of Chemistry, Faculty of Science, Mahidol University, Bangkok 10400, Thailand
[c] Institute of Science and Technology for Research and Development, Mahidol University, Salaya Campus, Nakorn Pathom 73170, Thailand

ARTICLE INFO

*Article history:*
Received 29 October 2008
Received in revised form 7 April 2009
Accepted 9 April 2009
Available online 22 April 2009

*Keywords:*
Chitosan
Silk fibroin
Blend films
Nanocomposite films
Nanoporous structures

ABSTRACT

Chitosan (CS)/silk fibroin (SF) blend films containing nanoparticles of methoxy poly(ethylene glycol)-*b*-poly(D,L-lactide) (MPEG-*b*-PDLL) were prepared by film casting of nanoparticle suspension–CS/SF blend solution. The nanocomposite blend films with CS/SF blend ratios of 2/0, 2/1, 2/2, 1/2 and 0/2 (w/w) were investigated. FTIR results showed the intermolecular bonds existed between nanoparticles and CS/SF film matrices. The nanoparticles with spherical shape observed from SEM micrographs were approximately less than 1 μm in size and dispersed throughout the film matrices. Nanopores on both film surfaces and cross-sections of the nanocomposite blend films were formed due to self-condensation and phase separation of the nanoparticles. The nanocomposite blend films contained nanoparticles exhibited an increase of film strength and decrease of film flexibility and water wettability.



## 1. Introduction

Chitosan (CS) and silk fibroin (SF) are polysaccharide and fibrous protein biopolymers, respectively, that have received great attention in medical and pharmaceutical applications because of their biodegradability and biocompatibility (Altman et al., 2003; Muzzarelli & Muzzarelli, 2005; Ravi Kumar, Muzzarelli, Muzzarelli, Sashiwa, & Domb, 2004). The CS shows excellent film-forming property whereas the SF film is very brittle and difficult to handle. However, the SF matrices have been found to be excellent cell adhesion, cell proliferation and enzyme immobilization materials (Kim, Kim, Vunjak-Novakovic, Min, & Kaplan, 2005; Meinel et al., 2005). Improvement of SF film flexibility by blending with CS has been reported in a few works (Chen, Li, & Yu, 1997; Park, Lee, Ha, & Park, 1999).

The nanoporous films have tremendous potential applications such as optical storage media, biosensors, templates, catalysis and size-/shape-selective separation media (You, Wen, Zhou, Wu, & Zhao, 2008). The nanoporous CS films have been prepared for use as metal absorbent (Liu, Tang, Chen, & Xin, 2005). In previous works (Baimark, Niamsa, Morakot, Threeprom, & Srisuwan, 2007a; Khamhan, Baimark, Chaichanadee, Phinyocheep, & Kittipoom, 2008), nanocomposite CS films loading with nanoparticles of methoxy poly(ethylene glycol)-*b*-poly(ε-caprolactone) (MPEG-*b*-PCL) have been reported. The nanoparticles dispersed throughout the CS film matrices enhanced water vapor sensitivity due to a hydrophobic character of MPEG-*b*-PCL nanoparticles. The nanocomposite CS films showed nanoporous structures throughout the CS film matrices. The nanoporous structures were also produced when the SF was used as the film matrix instead of CS (Srisuwan et al., 2008). The effect of CS/SF blend film matrices on nanopore morphology and nanocomposite film properties was also investigated.

In this research, nanocomposite CS/SF blend films containing methoxy poly(ethylene glycol)-b-poly(D,L-lactide) (MEPG-*b*-PDLL) nanoparticles were prepared. Functional groups and its intermolecular interactions were studied by FTIR spectroscopy. Influence of CS/SF blend ratios on film characteristics including film morphology, mechanical properties, water wettability and moisture uptake were investigated.

## 2. Materials and methods

### 2.1. Materials

Chitosan (CS) with 90% deacetylation and molecular weight of 80 kDa was purchased from Seafresh Chitosan Lab Co., Ltd. (Thailand) and used without further purification. About 1% (v/v) acetic acid aqueous solution was used as a solvent to prepare 1% (w/v) chitosan solution. Silk fibroin (SF) aqueous solution was prepared by a chemical degummed method and dissolved before dialysis, respectively, as follows. Cocoons from *Bombyx mori* were degummed by boiling twice in 0.5% $Na_2CO_3$ solution at 98–100 °C

* Corresponding author. Tel./fax: +66 43 754246.
*E-mail address:* yodthong.b@msu.ac.th (Y. Baimark).

0144-8617/$ - see front matter © 2009 Elsevier Ltd. All rights reserved.
doi:10.1016/j.carbpol.2009.04.003

**Table 1**
Formulations of nanocomposite CS/SF blend films.

| Film No. | 1% (w/v) CS solution (mL) | 1% (w/v) SF solution (mL) | MPEG-*b*-PDLL/CS/SF (w/w/w) |
|---|---|---|---|
| 1 | 21 | – | 0.05/0.21/0 |
| 2 | 14 | 7 | 0.05/0.14/0.07 |
| 3 | 10.5 | 10.5 | 0.05/0.105/0.105 |
| 4 | 7 | 14 | 0.05/0.07/0.14 |

for 30 min to remove sericin, then rinsed with distilled water and dried at room temperature. Degummed SF fibers were dissolved in $CaCl_2$–ethanol–water system (mole ratio = 1:2:8), by stirring at 80 °C for 2 h. The resulting SF solution was then dialyzed with cellulose tube for 3 days against distilled water. The distilled water was refreshed every day. The final concentration after dialysis was adjusted to 1% (w/v) with distilled water.

Methoxy poly(ethylene glycol)-*b*-poly(D,L-lactide) diblock copolymer (MPEG-*b*-PDLL) with number-average molecular weight and molecular weight distribution of 73,600 g/mol and 1.88, respectively, was synthesized as previously described (Baimark, Srisa-ard, Threeprom, Molloy, & Punyodom, 2007b). MPEG with molecular weight of 5000 g/mol and stannous octoate were used as an initiating system. The obtained MPEG-*b*-PDLL was completely amorphous state. All solvents in analytical grade were used.

### 2.2. Preparation of nanocomposite blend films

Nanocomposite CS/SF blend films containing MPEG-*b*-PDLL nanoparticles were prepared by film casting of MPEG-*b*-PDLL nanoparticle suspension–CS/SF blend solution. The surfactant-free MPEG-*b*-PDLL nanoparticles were firstly formed in the blend solution by the modified-spontaneous emulsification solvent diffusion (modified-SESD) method (Baimark, Srisa-ard, Threeprom, & Narkkong, 2007c). This procedure was explained as follows. About 2 mL of 2.5% (w/v) MPEG-*b*-PDLL solution in 3/3 (v/v) acetone/ethanol mixture was added drop-wise into the blend solution with stirring at 600 rpm. The organic solvents were evaporated in a fume hood for 6 h. Then, colloidal nanoparticles of MPEG-*b*-PDLL in blend solution was obtained and poured on Petri dish and left for drying at 40 °C during 24 h. The formulations of each nanocomposite blend film are summarized in Table 1. The blend films with CS/SF ratios of 2/0, 2/1, 2/2, 1/2 and 0/2 (w/w) were prepared as the same method for comparison.

### 2.3. Characterization of nanocomposite blend films

Chemical structures of the films were analyzed by FTIR spectroscopy using a Perkin–Elmer Spectrum GX FTIR spectrometer. The resolution of 4 $cm^{-1}$ and 32 scans were chosen in this work.

Surface and cross-section morphologies of the films were investigated by scanning electron microscopy (SEM) using a JEOL JSM-6460LV SEM. The film cross-section was obtained after cutting film with paper–scissors. Prior to examination, the sample films were sputter-coated with gold for enhancing surface conductivity.

Tensile strength and elongation at break of the films were preformed by tensile tester using an Instron Model 4301 Universal Testing Machine with 50% ± 5% relative humidity (RH). The films with 10 × 25 mm in size were tested with a speed of 50 mm/min and 1 kN load cell. The tensile strength and elongation at break were calculated as follows.

$$\text{Tensile strength at break } (N/mm^2) = \frac{\text{Breaking force } (N)}{\text{Cross-section area of the sample } (mm)^2} \quad (1)$$

$$\text{Elongation at break } (\%) = \frac{\text{The increase in length at breaking point } (mm) \times 100}{\text{Original length } (mm)} \quad (2)$$

Contact angles between water and films were measured at room temperature by using a Krüss DSA 10 Contact Angle Meter. Water was carefully dropped onto chitosan films and contact angles were quickly determined before the films commenced to swell. The reported values are an average of five different measurements.

Percent moisture uptake of the films was determined by the method previously described (Khamhan et al., 2008). Briefly, the sample films with 20 × 20 mm in size were dried in vacuum oven at room temperature for a week before weighing. They were then kept in a desiccator with 90% ± 5% RH maintained with a saturated sodium chloride solution at 30 ± 2 °C. The sample films were weighed again after being kept in the desiccator for 48 h. The moisture uptakes were an average of three different determinations. Percent moisture uptake was calculated as follow.

$$\%\text{Moisture uptake} = [(M_r - M_i)/M_i] \times 100 \quad (3)$$

where $M_i$ and $M_r$ are the initial and final weights (g) of the films, respectively.

## 3. Results and discussion

### 3.1. FTIR analysis

The preparation and characterization of CS/SF blend films have been published by a few researchers (Chen et al., 1997; Park et al., 1999). In these researches, FTIR has been used to study the hydrogen intermolecular bonding between CS and SF. Conformational transition from random coil to β-sheet conformation of the SF was induced by blending with CS (Chen et al., 1997). Fig. 1 shows FTIR spectra of the CS/SF blend films. The FTIR spectrum of CS film in Fig. 1(a) shows absorption bands at 1660, 1556, 1409 and 1070 $cm^{-1}$ assigned to polysaccharide structure (Wang & Li, 2007). The FTIR spectrum of SF film in Fig. 1(e) presents absorption bands at 1678 (amide I), 1575 (amide II) and 1237 (amide III), which attributed to the random coil conformation. The amide I bands of SF were slightly shifted to lower wave number when blending with CS, as shown in Figs. 1(b)–(d). The β-sheet amide I SF band is found at a lower wave number than its random coil form. This indicated that the SF conformation was changed from random coil to β-sheet form by blending with CS according to the literatures (Chen et al., 1997; Park et al., 1999). In addition, the bands at 1070 and 1237 $cm^{-1}$ of CS and SF characteristics, respectively, were slightly shifted from their pure films, supporting an occurrence of intermolecular interactions between CS and SF in the blend films.

Fig. 2 shows FTIR spectra of MPEG-*b*-PDLL nanoparticles-loaded nanocomposite CS/SF blend films. It can be seen that the absorption bands in the range of 1766–1755 $cm^{-1}$ attributed to carbonyl groups of MPEG-*b*-PDLL were existed. This band was slightly shifted for the blend films suggested that the intermolecular bonding had occurred between nanoparticles and CS/SF matrices. This may be expected as the intermolecular bonds between carbonyl groups of MPEG-*b*-PDLL and amino groups of CS/SF film matrices.

### 3.2. Morphology study

Film morphology was determined from SEM micrographs of film surface and cross-section. The film surfaces and cross-sections of all blend films were smooth without phase separation as an example of which is shown in Fig. 3 for 1/1 (w/w) CS/SF blend film.

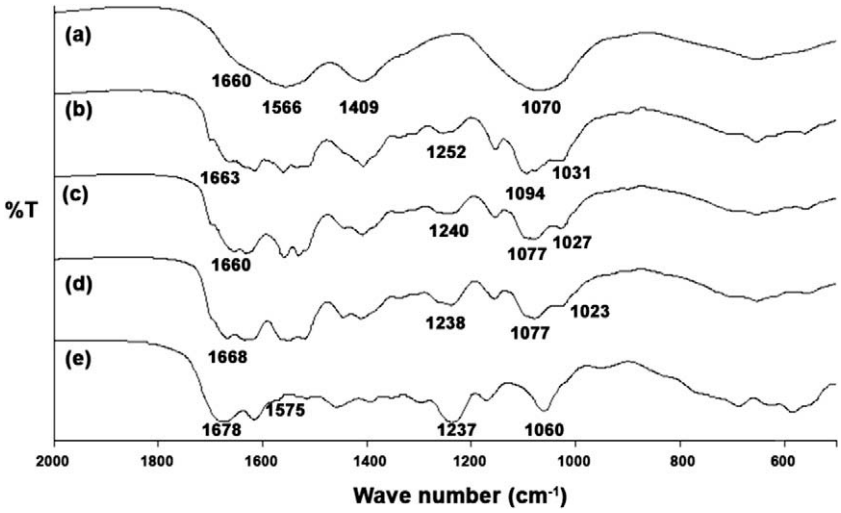


**Fig. 1.** FTIR spectra of CS/SF blend films with blend ratios of (a) 2/0, (b) 2/1, (c) 2/2, (d) 1/2 and (e) 0/2 (w/w).

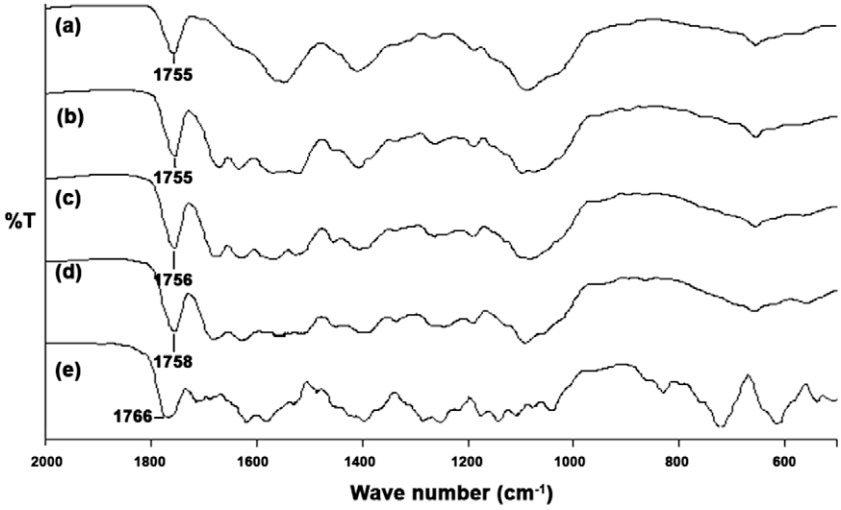


**Fig. 2.** FTIR spectra of nanocomposite CS/SF blend films with blend ratios of (a) 2/0, (b) 2/1, (c) 2/2, (d) 1/2 and (e) 0/2 (w/w).

Figs. 4 and 5 show SEM micrographs of the film cross-sections and their expansion, respectively. All film thicknesses observed from Fig. 4 were approximately 25 μm. The film cross-sections of nanocomposite blend films were rougher than the blend films. The MPEG-*b*-PDLL nanoparticles in the nanocomposite blend films were dispersed throughout the blend film matrices. These nanoparticles with less than 1 μm in size can be clearly observed from the expanded SEM micrographs as shown in Fig. 5.

In addition, nanopores were also observed throughout the film matrices (Fig. 5), which suggested that the nanocomposite blend films contained nanoporous structures. The nanopores in CS and SF nanocomposite films were formed due to self-condensation and phase separation of the nanoparticles (Baimark et al., 2007a; Srisuwan et al., 2008). However, the nanopore sizes of the nanocomposite CS/SF blend films were larger than both CS and SF nanocomposite films (Fig. 5). This indicated that the CS and SF components in the blend film matrices affected to phase separation of nanoparticles during the film drying process. The film surfaces of the nanocomposite blend films also showed the nanopores but smaller in diameter than the film cross-sections as an example of which is shown in Fig. 6 for the nanocomposite 1/1 (w/w) CS/SF blend film. The molecules of oxygen, cell nutriments or other may be able to pass through these nanopores in wound dressing and cell culture applications.

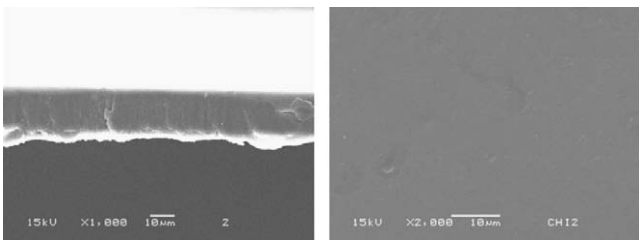


**Fig. 3.** SEM micrographs of film cross-section (left) and surface (right) of 1/1 (w/w) CS/SF blend film.

### 3.3. Mechanical properties

The mechanical properties of the films were studied from tensile stress–strain curves as shown in Figs. 7 and 8 for the blend and the nanocomposite blend films, respectively. The results of mechanical properties including tensile strength at break, elongation at break and initial Young's modulus are summarized in Table 2. The pure SF and nanocomposite SF films were very brittle and

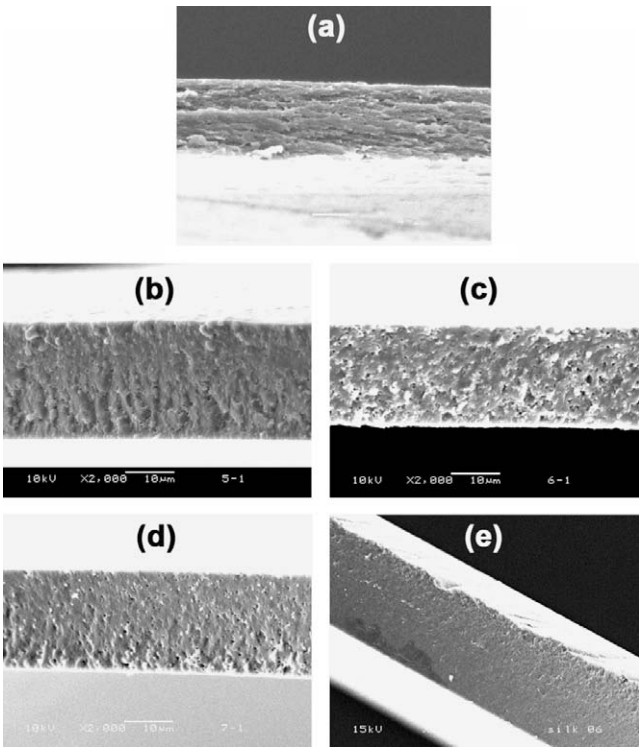


**Fig. 4.** SEM micrographs of film cross-sections of nanocomposite blend films with CS/SF weight ratios of (a) 2/0, (b) 2/1, (c) 2/2, (d) 1/2 and (e) 0/2 (bar = 10 μm).

difficult to cut as rectangle shape. Then, their tensile testing did not be performed. All nanocomposite blend films can be cut by paper–scissors into rectangle shape for tensile testing, suggesting that they were more flexible than the SF and nanocomposite SF films.

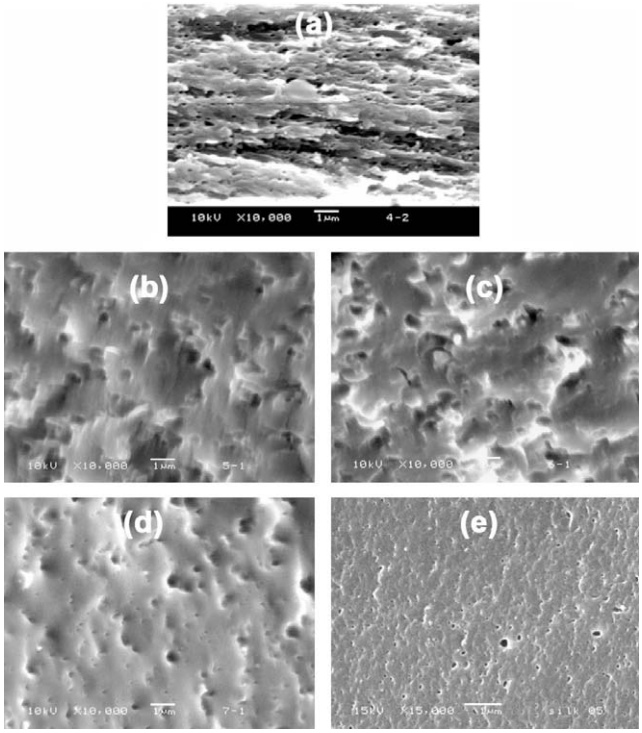


**Fig. 5.** Expanded SEM micrographs of film cross-sections of nanocomposite blend films with CS/SF weight ratios of (a) 2/0, (b) 2/1, (c) 2/2, (d) 1/2 and (e) 0/2 (bar = 1 μm).

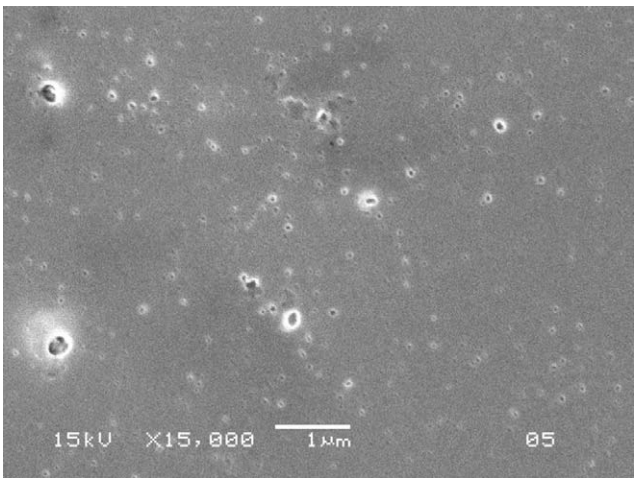


**Fig. 6.** SEM micrograph of film surface of nanocomposite 1/1 (w/w) CS/SF blend film (bar = 1 μm).

The stress–strain curves of the blend films in Fig. 7 shows an increase in tensile stress and initial Young's modulus and a decrease in elongation at break when SF blend ratio was increased, indicating that blending SF rendered the films less flexible due to the hardness characteristic of the SF. The nanoparticle-containing CS/SF blend films also exhibited an influence on the mechanical properties (Fig. 8), i.e. the tensile strength and the initial Young's modulus increased and the elongation decreased. These results may suggest that the nanoparticles could act as a reinforcing filler of the blend films. The interactions between nanoparticles and film matrices were confirmed by FTIR results as described above.

### 3.4. Water contact angles

Hydrophilicity of film surfaces were studied from water wettability. The water contact angle on film surfaces was determined for this purpose. The higher degree of water contact angle is directly related to lower surface hydrophilicity. Fig. 9 shows water contact angle results of both blend and nanocomposite blend films. The water contact angles of blend films increased as the SF blend ratio increased, suggesting that the SF component enhanced surface hydrophobicity of the blend films. However, the hydrophobic characteristics of the film surfaces also slightly increased when the nanoparticles were dispersed into the blend films due to their hydrophobic character.

### 3.5. Moisture uptakes

Hydrophobic biodegradable polylactide has been blended with the chitosan to improve water vapor resistance (Suyatma, Copinet,

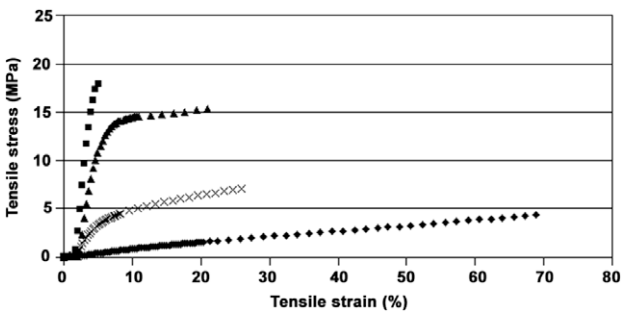


**Fig. 7.** Stress–strain curves of blend films with CS/SF blend ratios of (♦) 2/0, (×) 2/1, (▲) 2/2 and (■) 1/2 (w/w).

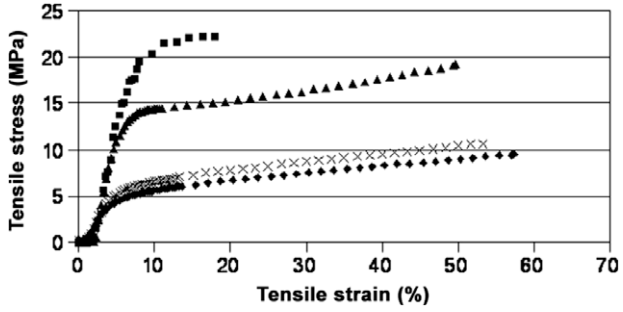


**Fig. 8.** Stress–strain curves of nanocomposite blend films with CS/SF blend ratios of (♦) 2/0, (×) 2/1, (▲) 2/2 and (■) 1/2 (w/w).

**Table 2**
Mechanical properties of blend and nanocomposite blend films.

| Film sample | CS/SF blend ratio (w/w) | Tensile strength (MPa) | Elongation (%) | Initial Young's modulus (MPa) |
|---|---|---|---|---|
| Blend films | 2/0 | 4.4 | 69 | 0.08 |
| | 2/1 | 6.9 | 27 | 0.76 |
| | 2/2 | 15.9 | 23 | 3.66 |
| | 1/2 | 18.0 | 5 | 5.36 |
| Nanocomposite blend films | 2/0 | 9.5 | 57 | 0.8 |
| | 2/1 | 10.6 | 54 | 1.3 |
| | 2/2 | 19.2 | 50 | 3.8 |
| | 1/2 | 22.2 | 18 | 3.9 |

Tighzert, & Coma, 2004). In this work, the presence of hydrophilic MPEG block was considered to enhance moisture sensitivity of the nanocomposite films, whereas hydrophobic PDLL block imparts an opposite property. The moisture uptakes of blend and nanocomposite blend films were measured instead of water uptake (immersion in water) because of the partial dissolution of CS and SF. Fig. 10 illustrates influences of the CS/SF blend ratios and the nanoparticle loading on the moisture uptakes of films. It was found that the moisture uptakes were directly related to the water contact angles. The moisture uptakes of the films decreased when the SF blend ratio was increased and the nanoparticles were incorporated into the films. This suggested that the hydrophobic characteristics of SF and nanoparticles exhibited resistant properties to moisture.

## 4. Conclusions

The nanocomposite blend films containing MPEG-*b*-PDLL nanoparticles with different CS/SF blend ratios were successfully prepared by film casting of the MPEG-*b*-PDLL nanoparticles suspension–CS/SF blend solution. First, the nanoparticles were prepared by the modified-SESD method in the blend solution. The intermolecular bonding between MPEG-*b*-PDLL and CS/SF were detected from FTIR spectra. The MPEG-*b*-PDLL nanoparticles, dispersed throughout the film matrices were approximately less than 1 μm in sizes with spherical shape. The nanocomposite blend films showed nanoporous structure. The nanoparticles dispersed in the blend films affected on an improved tensile strength at break and water/moisture sensitivity.

These biodegradable nanocomposite blend films may have potential for use in drug delivery, wound dressing and tissue engineering applications. The research on using these nanocomposite blend films for drug delivery application is under investigation.

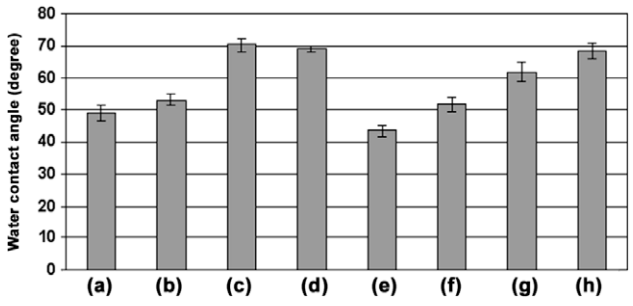


**Fig. 9.** Water contact angles of blend films with CS/SF blend ratios of (a) 2/0, (b) 2/1, (c) 2/2 and (d) 1/2 (w/w) and nanocomposite blend films with CS/SF blend ratios of (e) 2/0, (f) 2/1, (g) 2/2 and (h) 1/2 (w/w).

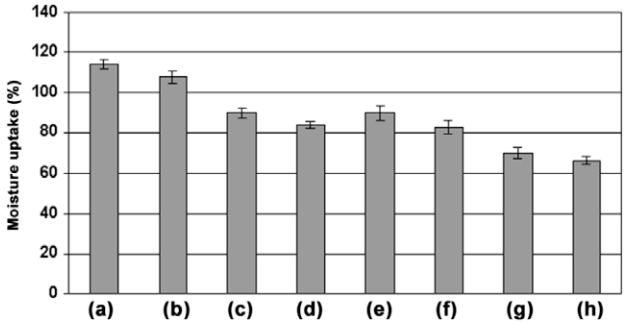


**Fig. 10.** Moisture uptakes of blend films with CS/SF blend ratios of (a) 2/0, (b) 2/1, (c) 2/2 and (d) 1/2 (w/w) and nanocomposite blend films with CS/SF blend ratios of (e) 2/0, (f) 2/1, (g) 2/2 and (h) 1/2 (w/w).

## Acknowledgements

The authors gratefully acknowledge Faculty of Science, Mahasarakham University, fiscal year 2008 and the Center of Excellence for Innovation in Chemistry (PERCH-CIC), Commission on Higher Education, Ministry of Education, Thailand for financial supports.

## References

Altman, G. H., Diaz, F., Jakuba, C., Calabro, T., Horan, R. L., Chen, J., et al. (2003). Silk-based biomaterials. *Biomaterials, 24*, 401–416.

Baimark, Y., Niamsa, N., Morakot, N., Threeprom, J., & Srisuwan, Y. (2007a). Preparation and morphology study of biodegradable chitosan/methoxy poly(ethylene glycol)-*b*-poly(ε-caprolactone) nanocomposite films. *International Journal of Polymer Analysis and Characterization, 12*, 457–467.

Baimark, Y., Srisa-ard, M., Threeprom, J., Molloy, R., & Punyodom, W. (2007b). Synthesis and characterization of methoxy poly(ethylene glycol)-*b*-poly(D,L-lactide-*co*-glycolide-*co*-ε-caprolactone) diblock copolymers: Effects of block lengths and compositions. *e-Polymers*, no. 138.

Baimark, Y., Srisa-ard, M., Threeprom, J., & Narkkong, N. (2007c). Preparation nanocolloids of methoxy poly(ethylene glycol)-*b*-poly(D,L-lactide): Effects of surfactant and organic solvent. *Colloid and Polymer Science, 285*, 1521–1525.

Chen, X., Li, W., & Yu, T. (1997). Conformation transition of silk fibroin induced by blending chitosan. *Journal of Polymer Science Part B: Polymer Physics, 35*, 2293–2296.

Khamhan, S., Baimark, Y., Chaichanadee, S., Phinyocheep, P., & Kittipoom, S. (2008). Water vapor permeability and mechanical properties of biodegradable chitosan/methoxy poly(ethylene glycol)-*b*-poly(ε-caprolactone) nanocomposite films. *International Journal of Polymer Analysis and Characterization, 13*, 224–231.

Kim, H. J., Kim, U.-J., Vunjak-Novakovic, G., Min, B.-H., & Kaplan, D. L. (2005). Influence macroporous protein scaffolds on bone tissue engineering from bone marrow stem cells. *Biomaterials, 26*, 4442–4452.

Liu, Y., Tang, J., Chen, X., & Xin, J. H. (2005). A templating route to nanoporous chitosan materials. *Carbohydrate Research, 340*, 2816–2820.

Meinel, L., Hofmann, S., Karageorgiou, V., Kirker-Head, C., McCool, J., Gronowicz, G., et al. (2005). The inflammatory responses to silk films in vitro and in vivo. *Biomaterials, 26*, 147–155.

Muzzarelli, R. A. A., & Muzzarelli, C. (2005). Chitosan chemistry: Relevance to the biomedical sciences. *Advance in Polymer Science, 186*, 151–209.

Park, S. J., Lee, K. Y., Ha, W. S., & Park, S. Y. (1999). Structural changes and their effect on mechanical properties of silk fibroin/chitosan blends. *Journal of Applied Polymer Science, 74*, 2571–2575.

Ravi Kumar, M. N. V., Muzzarelli, R. A. A., Muzzarelli, C., Sashiwa, H., & Domb, A. J. (2004). Chitosan chemistry and pharmaceutical perspectives. *Chemical Reviews, 104*, 6017–6084.

Srisuwan, Y., Srisa-ard, M., Sittiwet, C., Baimark, Y., Narkkong, N., & Butiman, C. (2008). Preparation and characterization of nanocomposite and nanoporous silk fibroin films. *Journal of Applied Science, 12*, 2258–2264.

Suyatma, N. E., Copinet, A., Tighzert, L., & Coma, V. J. (2004). Mechanical and barrier properties of biodegradable films made form chitosan and poly(lactic acid) blends. *Journal of Polymers and the Environment, 12*, 1–6.

Wang, L., & Li, C. (2007). Preparation and physicochemical properties of a novel hydroxyapatite/chitosan–silk fibroin composite. *Carbohydrate Polymers, 68*, 740–745.

You, B., Wen, N., Zhou, S., Wu, L., & Zhao, D. (2008). Facile method for fabrication of nanocomposite films with an ordered porous surface. *Journal of Physical Chemistry B, 112*, 7706–7712.